H1 LIQUID ARGON CALORIMETER ENERGY SCALE PROGRESS

JÜRGEN NAUMANN
Institut für Physik
Universität Dortmund
44331 Dortmund, Germany
E-mail: naumann@physik.uni-dortmund.de

The H1 Liquid Argon Calorimeter has been built with the aim to measure energies with scale uncertainties of 1% for electrons and photons and 2% for hadronic particles. In large parts of the calorimeter these design goals have now been reached using detailed offline studies which had become possible with the increased statistics of HERA *ep* data. Monitoring the liquid argon purity allows to study the time dependent stability of the energy scale. Therefore new attempts have been made to complement the determination of the argon purity in the calorimeter modules with muons.

1 Introduction

In the H1 Experiment [1] at HERA a Liquid Argon (LAr) Calorimeter is used to measure the energies of particles emerging from the interaction of 27.5 GeV electron (or positron) and 820 GeV (or 920 GeV) proton beams over an angular range of $4° \leq \theta \leq 154°$ [a].

The H1 Liquid Argon Calorimeter [2] is a non-compensating sampling calorimeter consisting of inner electromagnetic and outer hadronic sections. It is divided into 8 self supporting wheels each build out of 8 octants in the barrel part or two half shells in the forward part. In the electromagnetic modules lead is used as absorber material which adds up to 20 - 30 radiation length (X_0). The hadronic part is build out of stainless steel absorber plates which corresponds to 4.5 - 8 interaction lengths (λ) including the electromagnetic section.

2 Monitoring of Argon Purity

2.1 Charge Collection Efficiency

The sampling structure forms small ionisation chambers filled with liquid argon. A particle crossing the calorimeter ionizes the argon and a fraction of

[a] H1 uses a right-handed coordinate system, where the direction of the proton beam defines the positive z-direction. The polar angle θ is measured with respect to this direction.

the deposited charge $Q(U_{HV})$ is collected with a high voltage U_{HV} supplied across the argon gap. This fraction is called the charge collection efficiency ε (CCE). Assuming constant energy deposition along the particle track a phenomenological approach was found:

$$\varepsilon(U_{HV}) = \frac{Q(U_{HV})}{Q_0} = 2 \cdot \frac{\alpha\, U_{HV}}{p\, d_{Gap}^2} \left[1 - \frac{\alpha\, U_{HV}}{p\, d_{Gap}^2} \left(1 - e^{-\frac{p\, d_{Gap}^2}{\alpha\, U_{HV}}} \right) \right] \qquad (1)$$

where p [ppm] is the argon purity, d_{Gap} [cm] the readout gap width and $\alpha = 0.15$ ppm$\cdot$cm^2/kV in liquid argon. [3]

With a source of known charge deposition Q_0 the CCE and the argon purity can be monitored. Since 1991 a system of probes with α and β sources is used which are installed inside the cryostat but outside the calorimeter modules. To determine the CCE inside the readout structure also muons are used nowadays.

2.2 High Voltage Curves with Muons

About twice per year a set of special runs with beam-halo– (for the forward part) and cosmic–muons (for the barrel part) is taken with different high voltage settings in the LAr. In practice about 7 hours are needed to get sufficient statistics on tape. Since the muon signal is low (signal to noise ratio $\approx 1.5 - 3.0$), the standard zero suppression has to be switched off to get the complete signal. An exact pedestal determination is performed with random trigger events. Other detectors have to be used for track information and a cylinder around this track is extrapolated into the calorimeter. Only cell signals inside the cylinder are summed up to minimize the noise contribution. The cylinder radius has to be optimised to get the complete signal which is normalized to the track length through the LAr. In a "high voltage curve" (see Fig. 1) the mean normalized charge per track length is plotted versus the high voltage applied accross the LAr gap. Fitting equation 1 to the measured data gives the maximum available charge Q_0, the argon purity p and the CCE. This analysis is done for individual modules and provides local long term stability checks.

3 Energy Scale Studies with H1 Physics Data

Another method to improve the knowledge of the LAr calorimeter energy scale is to use physics data in offline analysis. With the increased amount of data collected in the past years the uncertainties in these studies had become smaller.

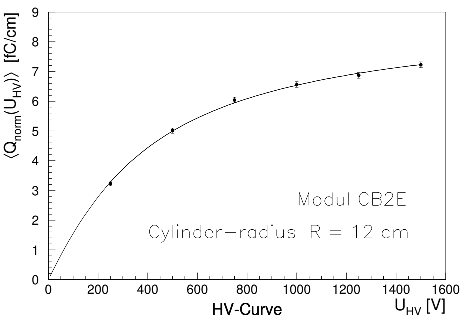

Figure 1. Mean charge deposited by muons crossing the calorimeter module CB2E (2-nd module in electromagnetic section of central barrel) normalized to track length through the liquid argon for different high voltage settings in the calorimeter readout gap. Cell signals inside a cylinder of 12 cm around the muon track are used.

3.1 Electromagnetic Energy Scale

An absolute calibration of the electromagnetic calorimeter sections requires an independent way to predict the particle energy.

For the backward part the well known kinematical cummulation (peak) in the energy distribution of the scattered e near electron beam energy can be used for calibration purpose. Comparing energy distributions for data and simulation an energy scale factor can be determined.

The reconstructing of particle decays, especially the $\pi^0 \rightarrow \gamma\gamma$ decay, can be used for energy correction in the lower energy range. The calibration can be checked by comparing the invariant mass spectrum in data and simulation [4].

The overconstrained kinematics of deep inelastic scattering (DIS) at HERA provide the possibility to predict the energy of a scattered electron from the electron beam energy and the scattering angles of the electron θ_e and the remaining final state θ with the double angle method (DA) [5]:

$$E_e(\theta_e, \theta) = \frac{2 \cdot E_{e-\mathrm{beam}} \cdot \sin\theta}{\sin\theta_e + \sin\theta - \sin(\theta_e + \theta)} \tag{2}$$

where the remaining final state can be a hadronic shower (DIS–DA) or a photon (QED-Compton–DA). Comparable is the ω–method [6], which is more robust against initial state radiation of the electron.

Using the latter two methods the increased amount of data provides a means now to calibrate the calorimeter with better precision. Events of the DIS sample where the electron is scattered under large angles are selected and

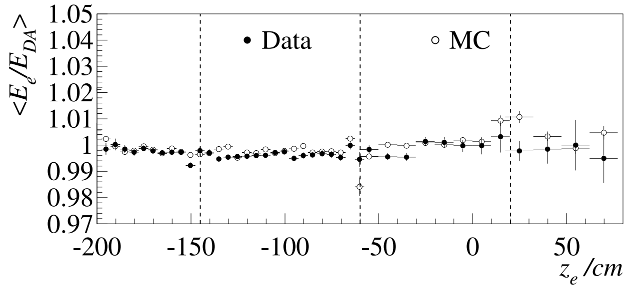

Figure 2. Ratio of electron energy E_e measured in the calorimeter and calculated with the double angle method (E_{DA}) as function of the impact point of the electron into the calorimeter. Larger deviations between data and simulation (MC) are near the cracks between calorimeter the modules. Positions of these cracks are marked with dotted lines.

the calculated electron energy using relation 2 is compared to the measured energy. With the present statistics this can be done for individual octants and fine z-bins as can be seen in Fig.2 where the ratio of measured to calculated energy is displayed versus the z-position of the electron impact point for data and simulation which are in good agreement. Deviations can be seen in cracks between the calorimeter modules and for larger z-values where the statistics gets lower.

In Fig.3 the results of the various methods are compared for the different electromagnetic calorimeter sections [7]. They are in good agreement among each other within the error bands which is $\pm$ 0.7 % in the central part and gets larger (up to $\pm$ 3 %) in the forward part due to lower statistics.

3.2 Hadronic Energy Scale

The hadronic energy scale can be adjusted with a relative calibration using the known electromagnetic energy scale and the balanced transverse momenta p_t of event final states. Correction factors are obtained from the ratio of transverse momenta of electron and hadronic final state.

The uncertainty of the hadronic energy scale is defined by the difference between the correction factors in data and Monte Carlo simulation. As can be seen in Fig.4, the uncertainties are below 2% in wide ranges of the calorimeter. There are larger deviations in the very backward part where mostly low energetic hadrons hit the calorimeter.

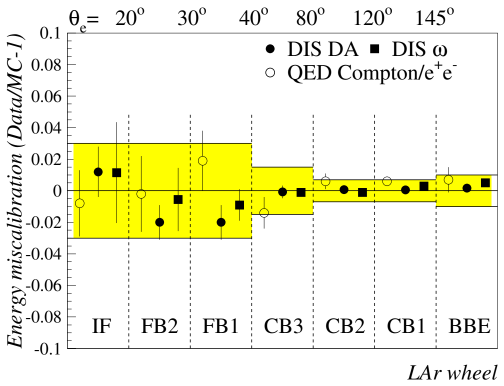

Figure 3. Calibration obtained with different methods in various parts of the calorimeter. Due to lower statistics the error band is larger in the forward part.

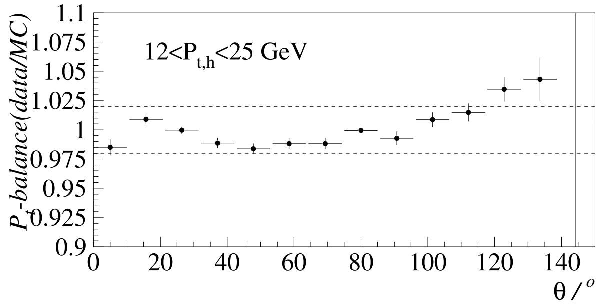

Figure 4. Relative difference between data and Monte Carlo simulation prediction for p_t-balance as a function of the mean hadronic scattering angle θ. In most parts the agreement is well within 2%. In the backward part deviations are larger due to low energetic hadrons.

3.3 Uncertainty of the Energy Scale

In Table 1 design goals for the energy scale uncertainties are compared to the results from two data analysis periods [7]. Using a luminosity of L=43.3 pb^{-1} collected between 1994 and 1997 it was possible to reach or even exceed the design goals in most calorimeter regions.

Table 1. Energy scale uncertainty in the H1 Liquid Argon Calorimeter: Given are the design goals and the scale uncertainties determined using different samples of physics data.

	Electromagnetic modules		Hadronic modules
	Central & backward	Forward	
Design goal	1%	1%	2%
1992-95 (L=9.7 pb^{-1})	1-2%	3%	4%
1994-97 (L=43.3 pb^{-1})	0.7-1.5%	3%	2%

4 Conclusion

With high voltage curves with muons a method has been developed which allows to determine the argon purity and the charge collection efficiency locally inside the H1 calorimeter modules. Offline studies using a large sample of physics data led to an improved understanding of H1 Liquid Argon Calorimeter energy scale. The uncertainties are compatible with the design goals or even below them in wide detector ranges.

Acknowledgments

I would like to thank the H1 Calorimeter Group and the Energy Scale Working Group for the hard work to provide stable detector operation and improved understanding of the calorimeter performance and for the opportunity to present our results in this very interesting conference for which I would like to thank the organizers as well.

Supported by BMBF under contract number 05 7Do 55 P.

References

1. H1 Collaboration, I. Abt *et al.*, *Nucl. Instrum. Methods* **A386**, 310 + 348 (1997)
2. H1 Calorimeter Group, B. Andrieu *et al.*, *Nucl. Instrum. Methods* **A336**, 460 (1993)
3. W. Hofmann *et al.*, *Nucl. Instrum. Methods* **135**, 151 (1976)
4. T. Wengler, *PhD Thesis, University of Heidelberg,* DESY-Thesis-1999-011 (1999)
5. S. Bentvelsen *et al.*, *Proceedings of the Workshop Physics at HERA, Vol. 1*, eds. W. Buchmüller, G. Ingelman, DESY (1992)
6. U. Bassler, G. Bernadi, *Z. Phys.* C **76**, 223 (1997)
7. H1 Collaboration, C. Adloff *et al.*, submitted to *Eur. Phys. J. C*